

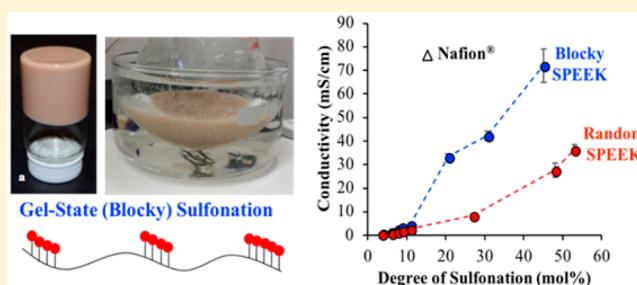
# Blocky Ionomers via Sulfonation of Poly(ether ether ketone) in the Semicrystalline Gel State

Lindsey J. Anderson,<sup>1</sup> Xijing Yuan,<sup>1</sup> Gregory B. Fahs,<sup>1</sup> and Robert B. Moore<sup>1\*</sup>

Department of Chemistry, Macromolecules Innovation Institute, Virginia Polytechnic Institute and State University, Blacksburg, Virginia 24061, United States

## Supporting Information

**ABSTRACT:** Blocky sulfonated poly(ether ether ketone) (SPEEK) ionomers were synthesized by postpolymerization functionalization in the gel state. Matched sets of blocky and random SPEEK with ion contents between 3 and 11 mol % were prepared, and the thermal transitions and crystallization kinetics were examined using differential scanning calorimetry (DSC). At similar ion contents, the blocky SPEEK exhibited higher crystallizability and faster crystallization kinetics than random SPEEK. Reduced scattering contrast in the USAXS/SAXS/WAXD analysis of the blocky SPEEK copolymer membranes, relative to the random analogues, suggested that the ionic aggregates in blocky SPEEK were distributed in close proximity to the crystalline domains. Despite similar water uptake values for the low ion content random and blocky SPEEK membranes, the blocky SPEEK exhibited higher proton conductivities than their random analogues. At significantly higher ion contents (45 mol %), the blocky SPEEK membranes remained semicrystalline, showed controlled water uptake, and exhibited a 2.5 times higher conductivity over that of the amorphous, random analogues. Moreover, these new blocky, semicrystalline SPEEK membranes were found to exhibit a proton conductivity that was comparable to that of the benchmark 1100 EW Nafion.



## INTRODUCTION

Fuel cells have emerged as a promising alternative energy candidate due to their high efficiency, renewable nature, and innocuous byproducts. A key component of fuel cells is the proton exchange membrane (PEM), which acts as both the proton conductor and the gas separator.<sup>1</sup> To function in the harsh environment of a fuel cell, PEMs must exhibit chemical and electrochemical stability, mechanical strength and integrity, and high proton conductivity.<sup>2–4</sup> The most widely studied PEM is Nafion, a perfluorinated ionomer that exhibits excellent thermal and mechanical stability in addition to exceptional transport properties.<sup>5–9</sup> The properties of Nafion arise from the phase separation of the hydrophobic poly(tetrafluoroethylene) (PTFE) backbone from the hydrophilic sulfonic acid groups, which generates a well-defined nano-separated morphology with a continuous hydrophilic domain. Despite its success as a benchmark PEM, Nafion has several drawbacks including high cost, difficult synthesis, and limited performance at high temperature and low humidity.<sup>10,11</sup> Thus, the search for novel low-cost, high-performance PEMs to replace Nafion has gained significant attention in recent years.<sup>12,13</sup>

Sulfonated aromatic hydrocarbon polymers such as poly(ether ether ketone)s, poly(ether sulfone)s, polyimides, and polybenzimidazoles have been explored as viable alternative PEMs due to their excellent mechanical properties, easy processability, and high hydrolytic, oxidative, and thermal

stability.<sup>14–16</sup> These materials are prepared by either postpolymerization sulfonation of the aromatic backbone or direct synthesis using sulfonated monomers. The degree of sulfonation dictates the ion exchange capacity of these membranes, and high degrees of sulfonation are necessary to achieve high proton conductivity.<sup>10</sup>

Among the widely explored hydrocarbon membranes, sulfonated poly(ether ether ketone) (SPEEK) is popular due to its low cost, ease of production, good proton conductivity, and high thermal and chemical stability.<sup>17–20</sup> Conventionally, SPEEK is prepared by postpolymerization functionalization using concentrated sulfuric acid.<sup>1,21,22</sup> Because of the limited solubility of PEEK, the sulfuric acid acts as both the solvent and the sulfonating reagent, resulting in heterogeneous sulfonation with a large distribution of sulfonic acid functionalities along the polymer chain. Using this method, the degree of sulfonation may be varied by sulfonation time and temperature; however, little control is granted over the ionic group distribution along the chains. In addition, the conventional method prohibits sulfonation below 20–30 mol % due to the concurrent dissolution and sulfonation of PEEK.<sup>23</sup>

Received: May 31, 2018

Revised: July 19, 2018

Published: August 7, 2018

To obtain better control over the ionic distribution along the polymer chains and enhance the properties of hydrocarbon membranes, amorphous block copolymers have been explored, wherein the hydrophilic sulfonic acid functionalities are concentrated into blocks along the polymer chain.<sup>24,25</sup> McGrath and co-workers synthesized block copolymers based on poly(arylene ether sulfone)s consisting of partially fluorinated ether sulfone blocks (hydrophobic block) and disulfonated ether sulfone blocks (hydrophilic block). These studies demonstrated that block copolymers have higher proton conductivity than random copolymers at similar ion contents due to improved hydrophobic/hydrophilic phase separation.<sup>26</sup> This enhanced performance was attributed to the fact that the multiblock architecture resulted in well-ordered lamellar morphologies with long-range periodicity. In contrast, the random architecture did not demonstrate any significant long-range order, and the ionic aggregates were poorly interconnected and homogeneously distributed throughout the amorphous polymer matrix.<sup>27</sup> McGrath also showed that block copolymers displayed enhanced proton conductivity at low hydration levels compared to random copolymers. Thus, it was postulated that a more interconnected network of hydrophilic domains is present in block copolymers as compared to random copolymers.<sup>28</sup> Other work has been performed to directly synthesize SPEEK block copolymers by controlled coupling of hydrophobic and hydrophilic oligomers.<sup>29,30</sup> Compared to random SPEEK, the synthetically tailored block copolymers of SPEEK exhibited increased proton conductivity and increased water uptake due to more well-defined phase separation.

Additional studies of directly synthesized poly(ether ether ketone)-disulfonated poly(arylene ether sulfone) block copolymers demonstrated that it is possible to preserve the semicrystalline nature of PEEK by separating the hydrophobic and hydrophilic domains into distinct blocks.<sup>31</sup> Again, the distinct nanophase morphology that arises in these block copolymers resulted in proton conductivities that were higher than Nafion 212 and the random copolymer analogues, even at low humidities. The incorporation of crystallinity into PEMs has also been shown to improve mechanical and thermal stability and decrease excessive swelling in water.<sup>13,32–34</sup> This is particularly important at the high degrees of sulfonation necessary to achieve good proton conductivity, where amorphous hydrocarbon membranes often swell or even dissolve in water.<sup>35</sup> Achieving a high degree of sulfonation with high crystallizability is advantageous to enable the production of membranes with good proton conductivity, mechanical durability, and resistance to undesirable swelling during PEM fuel cell operation.

Recently, we introduced a facile method of postpolymerization functionalization to produce “blocky” architectures.<sup>36,37</sup> This method consists of sulfonating semicrystalline, aromatic polymers in the semicrystalline gel state, as demonstrated using syndiotactic polystyrene (sPS). During sulfonation, the sulfonating reagent is sterically excluded from the tightly packed crystalline domains present in the gels and is only capable of reacting with the solvent-swollen amorphous chains within the physical network. Thus, selective sulfonation of the amorphous chain segments occurs, and long runs of unsulfonated, crystallizable sPS homopolymer are preserved. This method not only enables the synthesis of blocky copolymers using a simple experimental procedure but also conserves the crystallizability necessary for improved phase

separation and enhanced mechanical properties once the blocky materials are cast into membranes.

With our discovery of thermoreversible, semicrystalline gels of poly(ether ether ketone) (PEEK) in dichloroacetic acid (DCA),<sup>38</sup> it is now possible to extend the facile gel state functionalization method developed for sPS to other crystallizable polymers that are more suitable for PEM fuel cell applications. In this work, the sulfonation of PEEK gels was performed to produce SPEEK with a blocky architecture. The blocky SPEEK ionomers are compared to random SPEEK ionomers at similar degrees of sulfonation to determine the influence of ionic architectures on the resultant membrane properties. Relatively low degrees of sulfonation were examined in this initial report to highlight the effect of architecture on crystallizability, crystallization kinetics, and membrane properties.

## ■ EXPERIMENTAL SECTION

**Materials.** Poly(ether ether ketone) (PEEK) pellets (Victrex 150G) were obtained from Victrex. Dichloroacetic acid (DCA) was purchased from Sigma-Aldrich and was dried over magnesium sulfate (Fisher Scientific) and then filtered through a 0.45  $\mu\text{m}$  PTFE syringe filter prior to use. Trifluoroacetic anhydride was purchased from Sigma-Aldrich. Concentrated sulfuric acid (98%), 1,2-dichloroethane (DCE), sodium chloride, and cesium chloride were purchased from Fisher Scientific.

**Preparation of Sulfonating Reagent.** Trifluoroacetyl sulfate was prepared according to previously published procedures.<sup>39,40</sup> Trifluoroacetic anhydride (3.8 mL, 0.027 mol) was added to a nitrogen-purged round-bottom flask. The flask was cooled in an ice bath for 15 min, and then concentrated sulfuric acid (1 mL, 0.018 mol) was added. The solution was stirred vigorously for approximately 3 h to obtain a clear, light brown liquid.

**Random Sulfonation of Poly(ether ether ketone).** In contrast to the conventional method to sulfonate PEEK (i.e., heterogeneous dissolution and sulfonation in concentrated sulfuric acid), we have developed a procedure to first dissolve PEEK in a non-sulfonating solvent followed by a homogeneous sulfonation to obtain a truly random functionalization. PEEK (5.0 g) was dissolved in dichloroacetic acid at 185 °C to a final concentration of 10% w/v. Once dissolved, the temperature was decreased to 80 °C, and the solution was allowed to equilibrate at this temperature under nitrogen for 1 h. Next, 0.5–1 equiv of trifluoroacetyl sulfate was added dropwise to the PEEK solution, and the reaction was allowed to proceed for 1–4 h. For reactions targeting degrees of sulfonation of 15 mol % and above, reactions were run for up to 24 h. The reaction was terminated by precipitation into cold deionized water. The product was filtered, washed with deionized water, and then washed by Soxhlet extraction over methanol for 24 h. The resulting polymers were dried at 100 °C for 12 h. Prior to any analysis, samples were ground under liquid nitrogen to form a fine powder.

**Blocky Sulfonation of Poly(ether ether ketone).** PEEK (5.0 g) was dissolved in dichloroacetic acid at 185 °C to a final concentration of 20% w/v. Once dissolved, the solution was removed from heat and allowed to remain at room temperature for at least 24 h. During this time, the PEEK crystallizes from solution to form a thermoreversible gel network.<sup>38</sup> The gel was manually broken into small particles using a spatula and diluted to a 10% w/v suspension with additional dichloroacetic acid. For reactions targeting degrees of sulfonation higher than 15 mol %, the gel particles were diluted to a 10% w/v suspension in 1,2-dichloroethane (DCE). These reactions were performed for up to 48 h. The gel suspension was equilibrated at 80 °C under nitrogen for 1 h. Once equilibrated, 0.5–1 equiv of trifluoroacetyl sulfate was added dropwise to the PEEK solution, and the reaction was allowed to proceed for 1–4 h. The reaction was terminated by precipitation into cold deionized water. The product was filtered, washed with deionized water, and then washed by Soxhlet extraction over methanol for 24 h. The resulting polymers

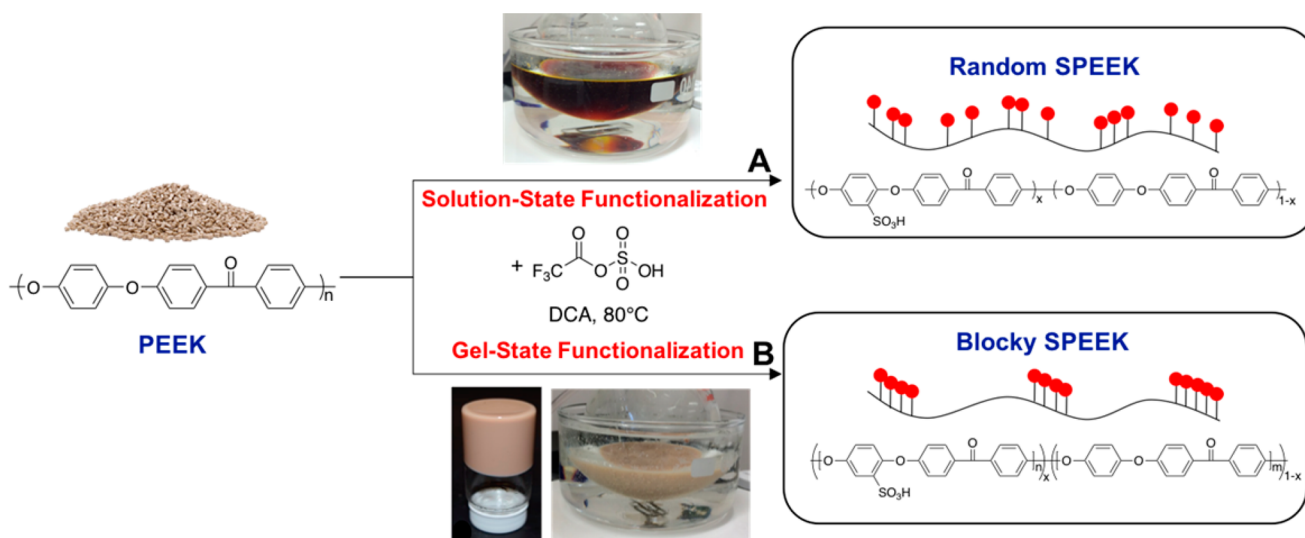


**Figure 1.** General synthesis of sulfonated poly(ether ether ketone). When performed in solution (A), a random or “statistical” copolymer is synthesized. When performed in the gel state (B), a blocky copolymer is synthesized due to the semicrystalline nature of the gel.

were dried at 100 °C for 12 h. Prior to any analysis, samples were ground under liquid nitrogen to form a fine powder.

**Membrane Preparation.** SPEEK membranes were prepared by dissolving the random or blocky SPEEK (in the H<sup>+</sup>-form) in DCA at 185 °C to a concentration of 15% w/v. Once dissolved, the solution was allowed to cool to room temperature and then filtered through a 0.45 μm PTFE syringe filter. These solutions were cast onto a glass substrate that was preheated to 100 °C using a doctor blade set to 7.5 mil. The wet films were allowed to dry on the heated substrate for 30 min, resulting in a final dry thickness of 25 μm. Membranes were washed with deionized water to remove residual DCA and then dried at 100 °C for 12 h.

**Ion Exchange.** The H<sup>+</sup>-form SPEEK samples were converted to the sodium-form (Na<sup>+</sup>-form) by stirring the powders in 2 M NaCl(aq) for 24 h. To convert to the cesium-form (Cs<sup>+</sup>-form), SPEEK samples (ground powders and/or cast membranes) were stirred in 1 M CsCl(aq) for 24 h. Samples in either salt form were then filtered, washed with deionized water to remove residual salt, and dried at 100 °C for 12 h. Complete ion exchange was confirmed by thermogravimetric analysis (see the [Supporting Information](#), Figure S1).

**<sup>1</sup>H NMR Spectroscopy.** <sup>1</sup>H NMR spectra were measured using a Bruker Avance III 600 MHz. Because of the low degree of sulfonation targeted for this study, conventional deuterated solvents were not able to dissolve the SPEEK samples, and thus a solvent suppression method was employed. SPEEK samples were dissolved in DCA at 185 °C to a concentration of 10% w/v. Once dissolved, the samples were cooled to room temperature and diluted by a factor of 5 using deuterated chloroform (CDCl<sub>3</sub>) with 0.05% v/v TMS. Presaturation of the intense DCA resonance at 6 ppm was performed during acquisition to obtain a suitable spectrum, free of a solvent contribution. The degree of sulfonation was calculated from the integration of the 10' peak relative to the combined area of the 1, 3, 6, and 8 peaks (see [Figure S2](#) for reference).<sup>1</sup> A full description of the chosen NMR solvent system is also described in the [Supporting Information](#), including Figures S3 and S4 and Table S1.

**Differential Scanning Calorimetry.** A TA Instruments Q2000 DSC was used to determine the thermal transitions and crystallization behavior of the SPEEK samples. Na<sup>+</sup>-form and Cs<sup>+</sup>-form SPEEK powders were used for this analysis, as acid-form SPEEK is not thermally stable at elevated temperatures.<sup>17,41</sup> Samples were predried at 150 °C for 5 min before several heating and cooling sequences. Under a nitrogen atmosphere, the dried samples (~5–8 mg) were heated from 0 to 380 °C at 20 °C/min, quench cooled to 0 °C, and then reheated from 0 to 380 °C at 20 °C/min. Furthermore, the isothermal crystallization was performed by heating SPEEK samples

from 25 to 380 °C at 20 °C/min, isothermally holding at 380 °C for 3 min, quench cooling to the desired crystallization temperature (*T<sub>c</sub>*), isothermally holding at this *T<sub>c</sub>* for 2 h, quench cooling to 100 °C, and finally heating from 100 to 380 °C at 10 °C/min. Isothermal crystallization was performed at 10 °C increments from 220 to 290 °C. The glass transition temperature (*T<sub>g</sub>*), enthalpy of crystallization ( $\Delta H_c$ ), melting temperature (*T<sub>m</sub>*), and enthalpy of melting ( $\Delta H_m$ ) were determined from each heat scan using the TA Instruments Universal Analysis software.

To evaluate the kinetics of crystallization, isothermal crystallization experiments were performed on the low degree of sulfonation Cs<sup>+</sup>-form SPEEK samples at various crystallization temperatures. Samples were ramped at 20 °C/min to 380 °C and were held at 380 °C for 3 min to completely melt the samples and eliminate thermal history. Samples were then cooled at 60 °C/min to the desired crystallization temperature and held at that temperature while measuring the exothermic heat of crystallization until no change in heat flow was observed. The crystallization half-time (*t*<sub>1/2</sub>) was determined at each isothermal crystallization temperature and was used as a measure of the rate of bulk crystallization for each sample.

**Water Uptake and Areal Swelling Ratio.** The water uptake and swelling ratios of the SPEEK (H<sup>+</sup>-form) membranes were determined by first drying membranes in a vacuum oven at 120 °C for 3 h. The mass (*W*<sub>dry</sub>) and dimensions (*L*<sub>*x*,dry</sub> × *L*<sub>*y*,dry</sub>) of the dry membranes were recorded. Then, the samples were treated in boiling deionized water for 1 h followed by equilibration in room temperature deionized water for 12 h. Membranes were blotted to remove excess surface water, and the mass (*W*<sub>wet</sub>) and dimensions (*L*<sub>*x*,wet</sub> × *L*<sub>*y*,wet</sub>) of the wet membranes were recorded. The water uptake and areal swelling ratio were calculated as

$$\text{water uptake} = \frac{W_{\text{wet}} - W_{\text{dry}}}{W_{\text{dry}}} \times 100\% \quad (1)$$

$$\begin{aligned} \text{areal swelling ratio} &= \frac{(L_{x,\text{wet}} \times L_{y,\text{wet}}) - (L_{x,\text{dry}} \times L_{y,\text{dry}})}{L_{x,\text{dry}} \times L_{y,\text{dry}}} \times 100\% \quad (2) \end{aligned}$$

The reported values are the average of four samples.

**Proton Conductivity.** Prior to analysis, SPEEK membranes were boiled in deionized water for 1 h and then soaked in room temperature deionized water for 12 h. In-plane proton conductivity was conducted using a four-point conductivity cell from Bekktech, which was immersed in deionized water at room temperature. Measurements were taken from 1 Hz to 1.5 MHz at a voltage

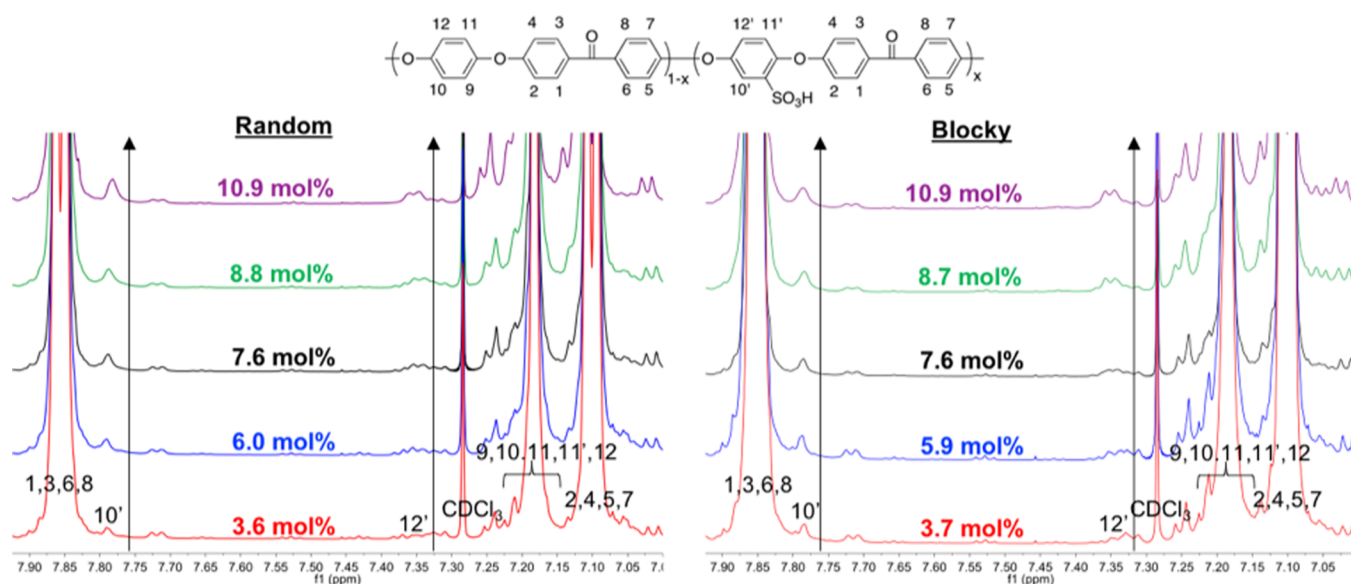


**Figure 2.** Solvent-suppressed  $^1\text{H}$  NMR of random and blocky SPEEK at various degrees of sulfonation.

amplitude of 50 mV using a 1255 HF frequency analyzer coupled to a 1286 electrochemical interface, both from Solartron Analytical. Data analysis was performed using the Zplot and Zview software from Scribner and Associates, Inc. The proton conductivity was calculated as

$$\sigma = \frac{1}{\rho} = \frac{l}{R \times A} \quad (3)$$

where  $\sigma$  ( $\text{S cm}^{-1}$ ) is the conductivity,  $\rho$  ( $\Omega\text{-cm}$ ) is the resistivity,  $l$  (cm) is the distance between the contacting electrodes,  $R$  ( $\Omega$ ) is the resistance determined from the real value of the complex impedance plot that corresponds to the minimum imaginary response, and  $A$  is the cross-sectional area of the membrane calculated from the width and thickness of the membrane. Measurements were performed on three separate membranes for each sample to ensure the reproducibility of results.

**USAXS/SAXS/WAXD Analysis.** Ultrasmall-angle X-ray scattering (USAXS), small-angle X-ray scattering (SAXS), and wide-angle X-ray diffraction data (WAXD) were collected at Argonne National Laboratory beamline 9ID-C, using a photon energy of 24 keV.<sup>42</sup> Scattering profiles are plotted as absolute intensity versus  $q$ , where  $q = \left(\frac{4\pi}{\lambda}\right) \sin(\theta)$ ,  $\theta$  is one-half of the scattering angle, and  $\lambda$  is the X-ray wavelength. USAXS measurements were performed using a Bonse-Hart camera. SAXS measurements were taken using the Pilatus 100k camera, and WAXD was collected using the Pilatus 100k-w camera. Data reduction was performed using the Irena<sup>43</sup> and Nika<sup>44</sup> data reduction software provided by Argonne. Scattering data were processed and corrected (1-dimensional data reduction, background subtraction, transmittance and thickness correction) using standard methods in the Nika software package.

## RESULTS AND DISCUSSION

**Synthesis of Random and Blocky SPEEK.** The sulfonation scheme of PEEK in both the homogeneous (solution state) and heterogeneous (gel state), using trifluoroacetyl sulfate, is shown in Figure 1. In the homogeneous solution state, all PEEK chains are completely solvated, making each repeat unit equally likely to be functionalized with the addition of sulfonating reagent. This results in a random or statistical SPEEK copolymer. In comparison, in the heterogeneous gel state, a physical network with two distinct domains exist: the solvent-swollen

amorphous fraction and the PEEK crystallites. During functionalization, the sulfonating reagent is sterically excluded from the tightly packed crystalline domains and thus is only capable of penetrating and functionalizing the solvent-swollen amorphous chains. This heterogeneous, gel state reaction process results in a blocky copolymer with pendent sulfonate units that are significantly concentrated into groups along the chains separated by relatively long runs of unfunctionalized, and thus crystallizable, PEEK segments.

To determine the effect of ionomer architecture (random versus blocky) on physical properties, a series of low degree of sulfonation SPEEK materials were prepared for each sulfonation method. A low degree of sulfonation was targeted to maintain a relatively high crystallizability for the SPEEK samples. Thereby, crystallizability may be used to probe the differences between blocky and random behavior in a manner similar to our low degree of sulfonation studies with syndiotactic polystyrene.<sup>36</sup> The  $^1\text{H}$  NMR spectra of the random and blocky functionalized SPEEK series are shown in Figure 2. Conventionally, the  $^1\text{H}$  NMR of SPEEK is performed in deuterated DMSO.<sup>22,45,46</sup> However, at the low degrees of sulfonation targeted in this work, SPEEK is not soluble in any polar aprotic solvents. Thus, a solvent suppression method using DCA and  $\text{CDCl}_3$  was developed (as described above) to obtain well-resolved spectra suitable for integration. As shown in Figure 2, degrees of sulfonation at 3.6, 6.0, 7.6, 8.8, and 10.9 mol % were obtained for the random SPEEK samples. The 10' and 12' peaks increase in intensity with increasing degree of sulfonation, thereby confirming that the regulation of time and reagent concentration is sufficient to yield control over low degrees of sulfonation using trifluoroacetyl sulfate.<sup>1</sup> In comparison, it is essentially impossible to achieve these low degrees of sulfonation using conventional sulfonation techniques, i.e., using sulfuric acid as both the solvent and sulfonation reagent, because a significant fraction of the PEEK chains are already highly sulfonated by the time the sample fully dissolves in sulfuric acid. A matched set of blocky SPEEK at 3.7, 5.9, 7.6, 8.7, and 10.9 mol % was also obtained for direct comparison to the random analogues. The  $^1\text{H}$  NMR spectra of the blocky samples displayed no

significant differences from the random samples. This is understandable because sulfonation occurs exclusively at one of the four sites on the electron-dense hydroquinone ring, regardless of architecture.<sup>47</sup> The naming of random and blocky ionomers will herein be represented by  $x$ SPEEK $z$ , where  $x$  signifies the architecture (R for random, B for blocky) and  $z$  is the molar degree of sulfonation.

**Thermal Analysis.** DSC was performed on the precipitated SPEEK samples to determine the influence of architecture on thermal transitions. As observed with sulfonated atactic polystyrene and sulfonated syndiotactic polystyrene, random architectures display a linear increase in  $T_g$  with increasing sulfonation while the  $T_g$  in blocky systems becomes independent of sulfonate content at high degrees of sulfonation.<sup>36,48,49</sup> Thus, analysis of the  $T_g$  versus degree of sulfonation provides indirect evidence of architecture in the SPEEK systems. The  $T_g$ 's as a function of degree of sulfonation for both the random and blocky SPEEK (in Cs<sup>+</sup>-form) are shown in Figure 3. As expected, sulfonation of PEEK leads to a

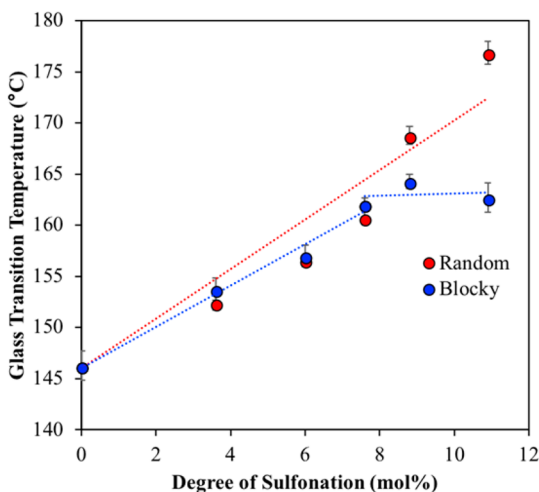


**Figure 3.** Glass transition temperature versus degree of sulfonation of random and blocky SPEEK copolymers in Cs<sup>+</sup>-form. Linear fits are provided as a visual guide.

higher  $T_g$  in the SPEEK samples due to a reduction in chain mobility from the physical cross-links formed by aggregation of the polar sulfonate groups. For degrees of sulfonation up to 7.6%, the random and blocky samples display similar  $T_g$ 's that increase with increasing degree of sulfonation. Above 7.6% sulfonation, the  $T_g$  of the random samples continues to increase up to 174 °C for RSPEEK10.9 while the  $T_g$ 's of the blocky samples remain constant at about 162 °C. The difference in  $T_g$  at higher degrees of sulfonation suggests that the gel state sulfonation process of PEEK leads to a blocky distribution of sulfonate groups.

DSC was also utilized to determine the effect of architecture on the crystallizability of SPEEK copolymers. SPEEK samples in Cs<sup>+</sup>-form were isothermally crystallized from the melt for 2 h at 250 °C. The DSC thermograms of PEEK, BSPEEK5.9, RSPEEK6.0, BSPEEK10.9, and RSPEEK10.9 and their respective degrees of crystallinity following isothermal crystallization at 250 °C are displayed in Figure 4. The degree of crystallinity,  $X_c$ , was determined using the relationship

$$X_c = \frac{\Delta H_f}{\Delta H_f^0} \quad (4)$$

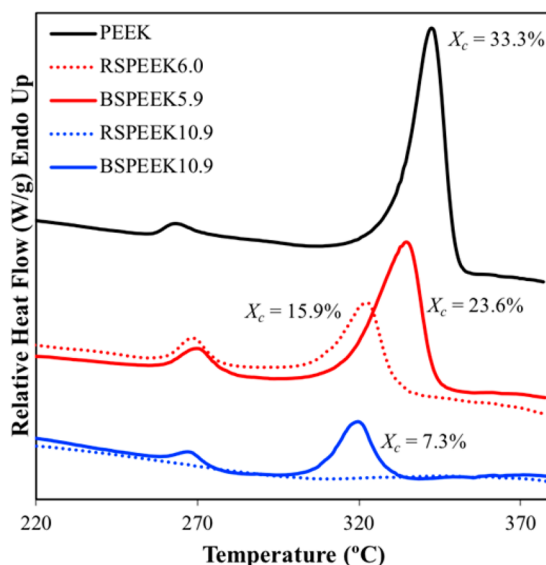


**Figure 4.** DSC thermograms of PEEK, RSPEEK6.0, BSPEEK5.9, RSPEEK10.9, and BSPEEK10.9 after isothermal crystallization for 2 h at 250 °C. All samples are in Cs<sup>+</sup>-form. The crystallinity of each sample is shown at their respective melting peak.

where  $\Delta H_f$  is the enthalpy of fusion determined from integration of the melting endotherm and  $\Delta H_f^0$  is the theoretical enthalpy of fusion of 100% crystalline PEEK (130 J/g).<sup>50</sup> Following isothermal crystallization, the PEEK homopolymer exhibits a double melting endotherm with a low melting temperature ( $T_{m1}$ ) of 265 °C and an upper melting temperature ( $T_{m2}$ ) of 342 °C. The double melting endotherm arises from two separate crystal populations that form during isothermal crystallization. The lower melting transition,  $T_{m1}$ , is attributed to thinner lamella formed during secondary crystallization while the upper melting transition,  $T_{m2}$ , is attributed to the main crystalline lamella formed during primary crystallization.<sup>51–53</sup> The  $T_{m1}$  is dependent on the crystallization temperature and generally lies 5–30 °C above  $T_c$ .<sup>52</sup> Because all SPEEK copolymers shown in Figure 4 were isothermally crystallized at 250 °C, the  $T_{m1}$  for all degrees of sulfonation and both architectures is approximately 268 °C, consistent with that of the PEEK homopolymer. The upper melting transition, however, is highly dependent on degree of sulfonation as well as architecture. At 6 mol % sulfonated, the BSPEEK5.9 ionomer exhibits a  $T_{m2}$  of 335 °C while RSPEEK6.0 exhibits a depressed  $T_{m2}$  of 322 °C. As expected, the  $T_{m2}$  values of both BSPEEK5.9 and RSPEEK6.0 both lie below that of the PEEK homopolymer due to melting point depression from the presence of noncrystallizable defects (i.e., sulfonated monomer units) in the copolymers. The melting point depression of RSPEEK6.0, however, is much more significant than that of BSPEEK5.9, suggesting that the blocky copolymer forms thicker primary crystalline lamella than its random analogue. Upon integration of the melting endotherm, it was also determined that the degree of crystallinity of BSPEEK5.9 ( $X_c = 23.6\%$ ) is significantly greater than that of RSPEEK6.0 ( $X_c = 15.9\%$ ).

The effect of defect sequencing along the SPEEK chain is amplified at higher degrees of sulfonation, where the random incorporation of noncrystallizable, interactive defects decreases the fraction of crystallizable runs and significantly lowers the equilibrium melting point of the copolymer, thus lowering the

crystallizability at low supercoolings.<sup>54–57</sup> At high degrees of sulfonation, it is observed that RSPEEK10.9 is completely amorphous following isothermal crystallization at 250 °C while BSPEEK10.9 displays the typical double melting endotherm of PEEK with an upper melting temperature of 320 °C and a crystallinity of 7.3%. Thus, the long runs of unfunctionalized, crystallizable homopolymer preserved by gel state sulfonation allows for the formation of thicker crystals during isothermal crystallization and a reduced effect of melting point depression consistent with nonrandom, “blocky” copolymers. The stark contrast in crystallizability between the random and blocky SPEEK is observed at a wide variety of crystallization temperatures, as shown in Figure S5. While these investigations have focused on crystallization from the melt, it is important to note that the as-precipitated SPEEK products (Table S2) exhibit much greater crystallinity due to solvation of the interactive ionic groups (and thus increased molecular mobility) in the presence of the polar solvent. Thus, a greater crystallizability is recognized for the as-cast membranes, which are prepared from a similar solution state.

**Isothermal Crystallization Kinetics.** To further elucidate the effect of ionomer architecture on the crystallization behavior of SPEEK, DSC isothermal crystallization experiments were performed. The kinetics of bulk crystallization of the matched sets of RSPEEK3.6 and BSPEEK3.7 and RSPEEK6.0 and BSPEEK5.9 in Cs<sup>+</sup>-form were analyzed using the following approach:

$$F_c(t) = \frac{\int_0^t \frac{dH}{dt} dt}{\int_0^\infty \frac{dH}{dt} dt} \quad (5)$$

where  $F_c(t)$  is the bulk fractional crystallinity of the functionalized copolymer systems that is equal to the heat evolved during isotherm crystallization at a specific time  $t$  divided by the total heat evolved during the entire isothermal crystallization process. For 3.7 mol % sulfonation, the samples were isothermally crystallized at 260, 270, 275, 280, and 290 °C. For 6.0 mol % sulfonation, the samples were isothermally crystallized at 220, 230, 240, 250, 260, and 270 °C. The plots of  $F_c(t)$  versus  $\ln(t)$  when crystallized at 260 °C are displayed in Figure 5. The crystallization isotherms for both architectures and degrees of sulfonation display a sigmoidal shape, which is characteristic of a nucleation and growth crystallization process. The shape of the isotherms are superimposable, suggesting no change in crystallization mechanism as an effect of degree of sulfonation or architecture. The rate of crystallization, however, is highly dependent on degree of sulfonation and architecture. As the degree of sulfonation increased from 3.7% to 6.0 mol %, both the random and blocky SPEEK displayed an increase in crystallization time (i.e., slower crystallization rate). However, at identical ion contents, the random samples displayed significantly longer crystallization time scales (i.e., over 2 orders of magnitude) than their blocky analogues. This effect was observed at all  $T_c$ 's, as shown in the Supporting Information (Figure S6).

The differences in crystallization kinetics between random and blocky ionomer architectures were further quantified by extracting the crystallization half-time,  $t_{1/2}$ , from the crystallization isotherms of Figure 5 and Figure S6. The analysis was also performed using the PEEK homopolymer for comparison, as shown in Figure 6. In addition, a full Avrami analysis of the results is shown in the Supporting Information (Table S3). At

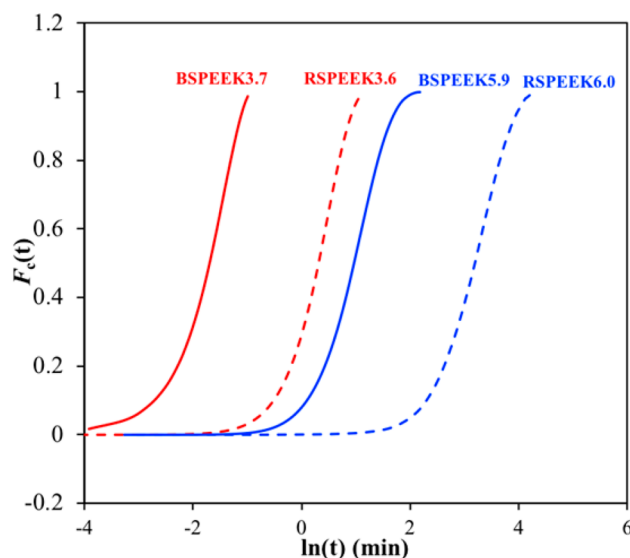


**Figure 5.** Bulk crystallization isotherms as fractional crystallinity versus  $\ln(t)$  for BSPEEK3.7, RSPEEK3.6, BSPEEK5.9, and RSPEEK6.0 crystallized at 260 °C.

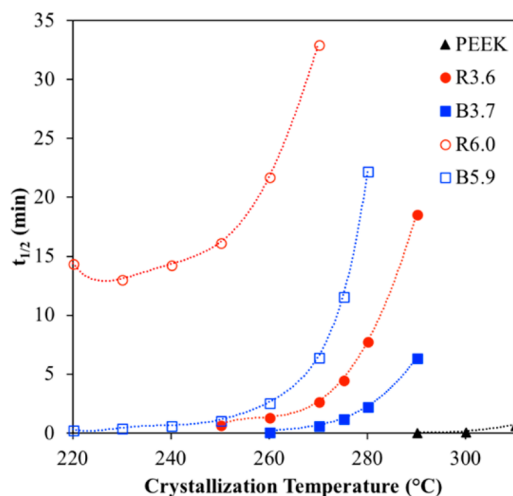


**Figure 6.** Crystallization half-time as a function of crystallization temperature for pure PEEK, RSPEEK3.6, BSPEEK3.7, RSPEEK6.0, and BSPEEK5.9. All SPEEK samples were in the Cs<sup>+</sup>-form.

3.7 mol % sulfonation, both the random and blocky SPEEK copolymers display higher crystallization half-times than pure PEEK. However, the BSPEEK3.7 has a smaller  $t_{1/2}$ , and thereby faster crystallization, than RSPEEK3.6 at all crystallization temperatures. The difference becomes even more distinct at high temperatures. For example, at 290 °C, the  $t_{1/2}$  for BSPEEK3.7 is more than 3 times shorter than the  $t_{1/2}$  for RSPEEK3.6 (i.e., 6 min versus 19 min). As the degree of sulfonation is increased to 6 mol %, the differences between the random and blocky architectures are even more pronounced. While BSPEEK5.9 is capable of crystallizing rapidly even at elevated temperatures, higher degrees of supercooling are necessary for RSPEEK6.0 to crystallize in under an hour ( $t_{1/2} < 30$  min). In fact, RSPEEK6.0 displays a minimum  $t_{1/2}$  value of 13 min at 230 °C while BSPEEK5.9 has a  $t_{1/2}$  value of 0.5 min at the same temperature.

At the temperatures investigated in Figure 6, the crystallization rates of PEEK, BSPEEK, and RSPEEK all

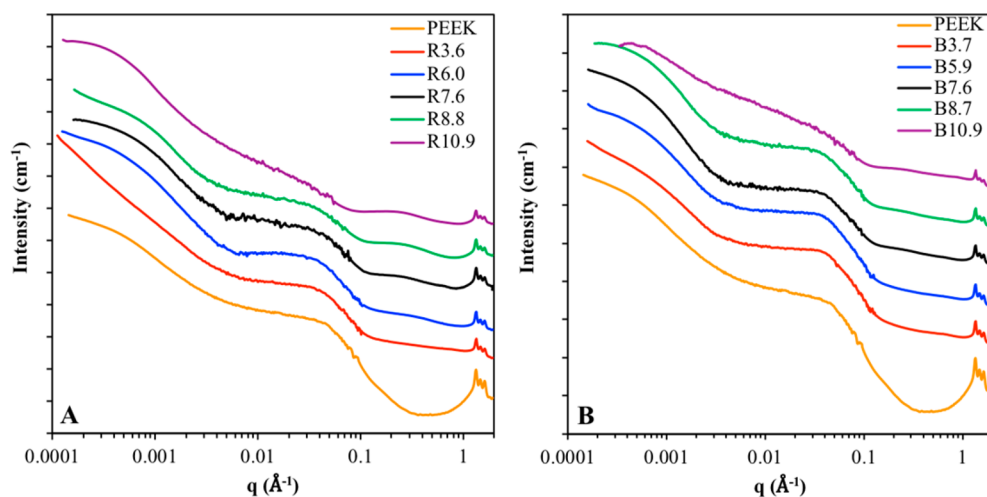


**Figure 7.** USAXS/SAXS/WAXD of random (A) and blocky (B) SPEEK membranes in Cs<sup>+</sup>-form. Scattering profiles have been vertically shifted for ease of viewing. For the random SPEEK membranes, peaks at 0.05 and 0.2 Å<sup>-1</sup> are clearly visible and are attributed to the semicrystalline structure and ionomer peak, respectively. For the blocky SPEEK membranes, only the semicrystalline peak at 0.05 Å<sup>-1</sup> is visible.

decrease with increasing  $T_c$ , as expected. This is indicative of a nucleation-controlled crystallization regime, thereby suggesting that the growth of crystallites is dependent on the ability of the crystallizable chain segments to establish and grow upon a crystal surface. It is important to note, especially for ionomers, that diffusion of chains segments within the melt also plays a significant role at these temperatures due to the presence of electrostatic interactions between the interactive (SPEEK) defects that restrict polymer chain mobility through ionic aggregation.<sup>57</sup> Consequently, the crystallization kinetics of these ionomers are slowed by both the rejection of defective stems (containing at least one sulfonated unit) from the growing crystal interface and by slower diffusion of the ionomer chain segments in the melt.

For the random SPEEK ionomers, the more homogeneous distribution of sulfonate groups along the polymer chain makes it more likely to encounter a sulfonated unit at the growing crystal surface (i.e., fewer runs of pure PEEK units of sufficient length to crystallize compared to the blocky analogue). This results in rejection of that defective chain segment from the crystal and thus a longer time period for bulk crystallization. For each ionic content, the prevalence of encountering a defective stem is greater for the random systems in comparison to the blocky analogue, where long runs of unfunctionalized homopolymer are maintained. Thus, blocky SPEEK ionomers are able to crystallize significantly faster than their random ionomer analogues due to a reduced prevalence of encountering a defective stem at the growing crystal interface.

**USAXS/SAXS/WAXD Analysis.** The morphological characterization of solution-cast membranes over a wide range of length scales was performed using USAXS/SAXS/WAXD at Argonne National Laboratories. The USAXS/SAXS/WAXD profiles of as-cast membranes of random and blocky SPEEK at all degrees of sulfonation as well as pure PEEK membranes are shown in Figure 7. All measurements were conducted on dry Cs<sup>+</sup>-form membranes to achieve enhanced contrast of the ionic domains. In the WAXD region (i.e.,  $q > 0.6 \text{ \AA}^{-1}$ ), all samples show diffraction peaks attributed to the characteristic interplanar reflections of the PEEK crystal structure. For both the random and blocky specimens, the intensity of the crystalline peaks is observed to decrease with increasing ion content (in agreement with the decreasing crystallizability with

ion content trend observed by DSC, above). While the RSPEEK10.6 was observed to be amorphous following isothermal crystallization from the melt (Figure 4), these WAXD data for solution-cast samples confirm that a significant degree of crystallinity can be developed in these low ion content SPEEK membranes during the solvent-borne casting process. Even the RSPEEK10.6 sample yields a degree of crystallinity of 18% when cast from DCA at 100 °C (Table S4).

In the USAXS region (i.e.,  $q < 0.006 \text{ \AA}^{-1}$ ), the SPEEK samples generally exhibit a broad exponential “knee” similar to that observed for the pure PEEK sample. The precise origin of this scattering feature requires further investigation (beyond the scope of this study); however, given that this knee is observed in pure PEEK, it is likely attributed to long-range heterogeneities in the spatial distribution of the PEEK crystalline domains.

In the SAXS region (i.e.,  $0.006 \text{ \AA}^{-1} < q < 0.6 \text{ \AA}^{-1}$ ), all of the samples show a distinct matrix knee at  $q \approx 0.05 \text{ \AA}^{-1}$  attributed to interlamellar scattering from the semicrystalline matrix.<sup>58</sup> To obtain an estimate of the lamellar dimensions from the interlamellar SAXS feature, the peak position of the scattering maximum for each sample was extracted from the Lorentz-corrected SAXS curve and was used to estimate the center-to-center intercrystalline domain spacing (i.e., long period) from Bragg’s law ( $d_{\text{Bragg}} = 2\pi/q$ ).<sup>59,60</sup> Note that the excess scattering contribution from the ion-rich domains (at  $q$  values larger than ca.  $0.05 \text{ \AA}^{-1}$ ; see below) precludes the use of a more accurate analysis of lamellar dimensions using a 1-D correlation function analysis.<sup>61</sup> By definition, the long period,  $L_p$ , is considered as the sum of the crystal lamellar thickness,  $l_c$ , combined with the thickness of the interlamellar amorphous region,  $l_a$ . Assuming a linear two-phase model, the  $l_c$  dimensions may be estimated for comparison by multiplying  $L_p$  by the volume fraction of crystallinity ( $\phi_c$ ) determined by XRD of the as-cast membranes, and the  $l_a$  dimensions may be determined by subtraction of  $l_c$  from  $L_p$ .<sup>50</sup> As shown in Table 1, the long periods for the ionomers are all greater than that of pure PEEK. This behavior is expected due to stastically shorter runs of crystallizable polymer chains for the SPEEK samples that tends to limit the lamellar thickness and increase  $l_a$ . Interestingly,  $L_p$  increases systematically with ion content for

**Table 1. SAXS Analysis of SPEEK Membranes**

sample	$q_{\max}$ ( $\text{\AA}^{-1}$ )	$L_p$ ( $\text{\AA}$ )	$\phi_c$	$l_c$ ( $\text{\AA}$ )	$l_a$ ( $\text{\AA}$ )
PEEK	0.046	137	0.40	55	82
RSPEEK3.6	0.044	143	0.28	40	103
BSPEEK3.7	0.044	143	0.30	43	100
RSPEEK6.0	0.041	153	0.25	38	115
BSPEEK5.9	0.042	150	0.27	41	109
RSPEEK7.6	0.040	157	0.24	37	120
BSPEEK7.6	0.042	150	0.26	40	110
RSPEEK8.8	0.040	157	0.21	33	124
BSPEEK8.7	0.042	150	0.26	39	111
RSPEEK10.9	0.031	203	0.16	32	171
BSPEEK10.9	0.042	150	0.22	33	117

the random SPEEK samples. In contrast, however,  $L_p$  remains constant at 150  $\text{\AA}$  for the blocky SPEEK samples having ion contents of 6 mol % and greater. By accounting for the differences in crystallinity between the blocky and random SPEEK samples, the linear two-phase approximation yields thicker  $l_c$  values and thinner  $l_a$  values, across the board, for the blocky SPEEK samples compared to the random SPEEK samples. Therefore, this comparative analysis further supports a blocky architecture and suggests that the crystalline dimensions attainable with the blocky SPEEK samples originate from a “memory” of the crystalline dimensions within the physical network during the gel state functionalization.

The SAXS region of the scattering profiles of Figure 7 also contains morphological information regarding contributions from the ionic component of these ionomers. At  $q$  values greater than  $0.1 \text{ \AA}^{-1}$ , it is clear that the SAXS scattering profiles of the SPEEK samples differ significantly from the featureless profile of the parent PEEK polymer. In agreement with previous SAXS studies of dry  $\text{Cs}^+$ -form SPEEK,<sup>58</sup> the excess SAXS scattering for these ionomers (over that of PEEK) is reasonably attributed to the ion-rich domains, which have a broad distribution of dimensions and relatively poor contrast with the semicrystalline matrix. With increasing ion content, the random SPEEK samples develop a distinct maximum, centered at  $q \approx 0.25 \text{ \AA}^{-1}$ , attributed to a feature characteristic of ionomers, known as the ionomer peak. For a broad class of ionomers, the ionomer peak has been attributed to the presence of nanophase-separated ionic aggregates (i.e., multiplets of ion pairs) that produce interparticle interferences that yield the characteristic scattering maximum.<sup>6</sup> For the random SPEEK samples, the ionomer peak increases in intensity with increasing degree of sulfonation and displays  $q$  values decreasing from 0.33 to  $0.22 \text{ \AA}^{-1}$  as the degree of sulfonation increases from 6.0 to 10.9 mol %. Using a Bragg estimate from the  $q_{\max}$  values (i.e.,  $d_{\text{Bragg}} = 2\pi/q_{\max}$ ), this yields an intermultiplet domain distance of 19–29  $\text{\AA}$ , which is consistent with previous studies of conventionally sulfonated SPEEK membranes in the literature.<sup>59,62,63</sup> Fitting of the ionomer peaks using a size distribution model with a spheroid form factor and hard sphere structure factor (details of the fitting process are described in the Supporting Information, Figures S7 and S8) shows that the multiplet radii of the random SPEEK membranes increase from 5.0 to 5.9  $\text{\AA}$  as the degree of sulfonation increases from 6.0 to 10.9 mol % (Table S5). Gebel and Gomes have similarly reported small ionic domains with radii of 4–6  $\text{\AA}$  for SPEEK membranes using various fitting procedures.<sup>58,64</sup> On the basis of this analysis, it is

evident that the random SPEEK ionomers are behaving as typical ionomers,<sup>6</sup> whereby both the size of the multiplets and the center-to-center distance between multiplets increase with degree of sulfonation.

In distinct contrast to the behavior of the random SPEEK samples, it is surprising to observe that a distinct ionomer peak is not present for the as-cast blocky SPEEK samples. The unexpected absence of an ionomer peak in the as-cast blocky SPEEK samples is further explored by comparing the scattering features of quenched samples of random and blocky SPEEK at 8.8 mol % sulfonation, as shown in Figure 8. For the quenched

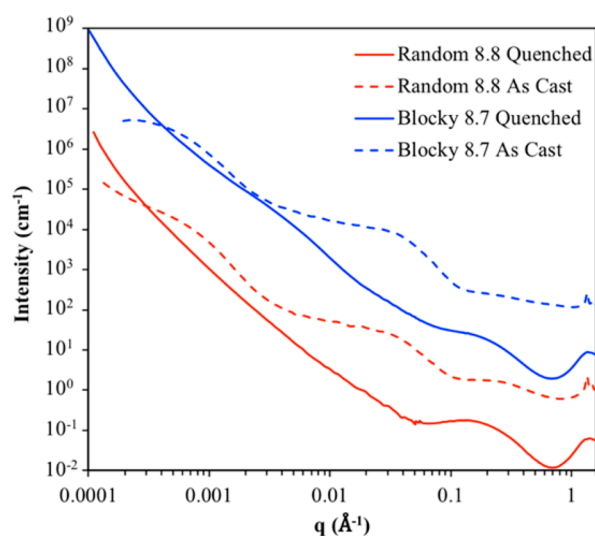


**Figure 8.** USAXS/SAXS/WAXS profiles of quenched RSPEEK8.8 (solid red), as-cast RSPEEK8.8 (dashed red), quenched BSPEEK8.7 (solid blue), and as-cast BSPEEK8.7 (dashed blue). Profiles have been shifted for ease of comparison.

samples, both the random and blocky SPEEK demonstrate one primary scattering feature—the ionomer peak at  $\sim 0.25 \text{ \AA}^{-1}$ . Fitting of these ionomer peaks using the method described above shows similar multiplet radii of the two architectures (6.7  $\text{\AA}$  for RSPEEK8.8 and 6.6  $\text{\AA}$  for BSPEEK8.7). Despite similar peak positions, the ionomer peak appears more prominent in the RSPEEK8.8 than in BSPEEK8.7. With the introduction of crystallinity (as shown by the as-cast membranes), the large crystalline shoulder at  $0.05 \text{ \AA}^{-1}$  appears and the ionomer peaks for both the random and blocky samples appear to decrease in intensity while shifting to higher  $q$ . By comparison, it is clear that the ionomer peak is essentially absent for the semicrystalline blocky SPEEK. In agreement with the work of Gebel,<sup>58</sup> the data in Figure 8 confirm that the intensity of the ionomer peak is diminished due to scattering contrast in the semicrystalline state (i.e., the electron density of the semicrystalline matrix is similar to the electron density of the ionic aggregates).

While the intensity of the ionomer peak in SPEEK is clearly affected by the limited contrast with the semicrystalline matrix, the apparent greater sensitivity to this scattering contrast for the blocky SPEEK may suggest that the ionic aggregates are more uniformly distributed in near proximity to the PEEK crystallites relative to the spatial distribution of aggregates and crystallites in the random analogue. While it is beyond the scope of this initial investigation into the gel-state sulfonation of PEEK, it is of interest to note that this phenomenon is not

unique to this blocky SPEEK. Our model blocky sulfonated syndiotactic polystyrene system<sup>36</sup> shows the same absence of an ionomer peak compared to the random analogue (Figure S9). Of course, further analysis will be required to determine the origin of this unanticipated scattering behavior. Nevertheless, it is intriguing to consider how this potentially altered distribution of ionic domains could affect the transport properties in membrane applications.

**Membrane Properties.** SPEEK is commonly employed as an alternative hydrocarbon proton exchange membrane for fuel cell applications.<sup>65–67</sup> While these applications require the use of materials with significantly higher degrees of sulfonation than that of the ionomer samples studied here, this initial comparison of membrane properties is used to represent the benefit of a blocky architecture in creating efficient conduction pathways and the impetus for expanding this facile, gel state synthetic scheme to higher degrees of functionalization. As shown in Figure 9, the water uptake of SPEEK membranes

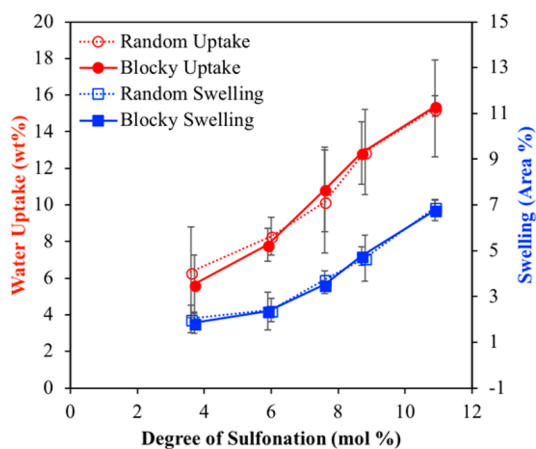


**Figure 9.** Water uptake and swelling of random and blocky SPEEK at various degrees of sulfonation.

(H<sup>+</sup>-form) increases as the degree of sulfonation increases. Likewise, the areal swelling increases with increasing degree of sulfonation. This effect is expected as increasing sulfonation

increases the number of hydrophilic ionic groups along the backbone. No difference is observed between the random and blocky SPEEK membranes at any degree of sulfonation, signifying that water uptake is independent of architecture at these low degrees of functionalization.

The proton conductivity of the SPEEK (H<sup>+</sup>-form) membranes immersed in water was also examined, as shown in Figure 10A,B. For the low degrees of sulfonation (Figure 10A), the blocky SPEEK membranes exhibit higher proton conductivities, across all degrees of sulfonation, relative to their random membrane analogues. Because proton conductivity is often observed to be directly correlated to the water content,<sup>68,69</sup> it is of interest to note that the blocky ionomers have higher conductivity than the random analogues despite having similar water uptake values. The degree of crystallinity for each of the membranes is also included for comparison next to each data point (the crystallinity values obtained by DSC and XRD are also listed in Table S4). By inspection, both the proton conductivity and the degree of crystallinity tend to diverge with increasing ion content. Given the similar water contents for the blocky and random analogues, this behavior may be attributed to the impact of crystallinity on the spatial distribution of the functional ionic groups within the amorphous phase of these membranes. As crystallinity develops during the casting process, this phase-separation phenomenon consequently increases the local concentration of ionic groups within the remaining amorphous phase. Because the blocky samples exhibit higher crystallinity than their random analogues, the local ion concentration in the amorphous phase is somewhat greater for the blocky SPEEK at similar ion contents.<sup>36</sup> Moreover, with a constant number of water molecules per sulfonate group, the consequence of a higher ion concentration for the blocky membranes implies that the blocky and random analogues have different local distributions of water within the ionic domains. Coupled with the SAXS analysis above, it may be reasonable to conclude that the hydrated ionic domains in the blocky membranes are more interconnected, providing for more efficient percolation pathways for proton and water transport. Future studies will focus on a systematic study of morphology–conductivity relationships over a range of water contents to probe this

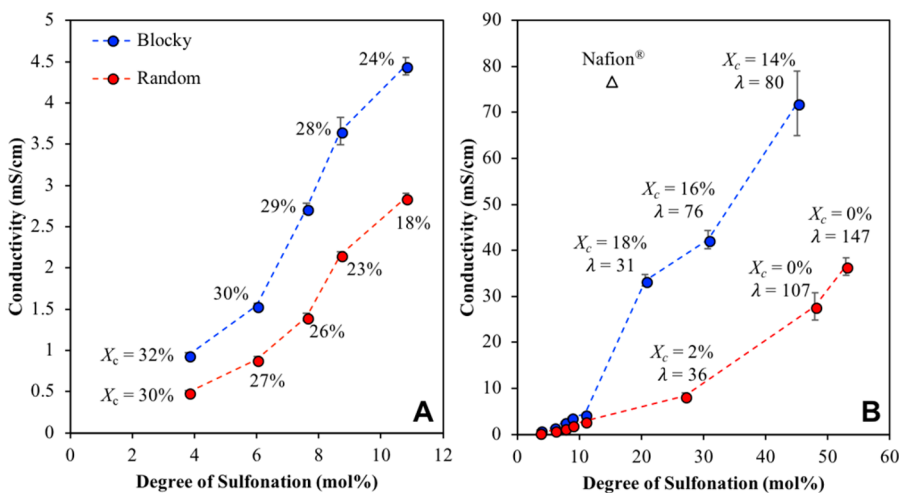


**Figure 10.** Proton conductivity of random and blocky SPEEK at various degrees of sulfonation. The  $X_c$  values displayed were determined using DSC, and  $\lambda$  (mol sulfonate/mol water) was determined using the water uptake. The open triangle represents the proton conductivity of the benchmark 1100 EW Nafion evaluated under identical conditions.

potential link between ionomer architecture and ionic domain connectivity.

To demonstrate the impact of a blocky ionomer architecture on SPEEK membranes containing ion contents relevant to PEMFC applications, the data in Figure 10B show conductivity results for SPEEK membranes having degrees of sulfonation exceeding 10 mol %. For comparison, the degrees of crystallinity ( $X_c$ ) and water content ( $\lambda$ ) values are listed next to each data point. As expected, the conductivities for all membranes continue to increase with degree of sulfonation. In addition, for these higher degrees of sulfonation, the water uptake is observed to increase as expected with ion content, and the values significantly diverge with the random SPEEK swelling much more than the blocky SPEEK. For a given degree of sulfonation, it is clear that the blocky architecture yields a profound increase in conductivity over that of a random analogue. This behavior is consistent with the results of other block ionomer membrane systems and further demonstrates the profound importance of “blocking up” the ions to achieve improved membrane performance.<sup>27,70</sup> Moreover, it is important to note that the blocky BSPEEK45 membrane has a room temperature conductivity value ( $\sigma = 72$  mS/cm) that is quite comparable to the conductivity of Nafion under the same conditions ( $\sigma = 77$  mS/cm). Furthermore, it is evident that by sulfonating in the semicrystalline gel state, a significant degree of crystallinity is retained that is unachievable in the random, solution state synthesis. The crystallinity of the blocky SPEEK not only imparts mechanical integrity to the membranes but also prevents excessive swelling at high degrees of functionality. For example, the RSPEEK53 membrane swells extensively ( $\lambda = 147$ ), near the point of dissolving and begins to break apart upon exposure to water. In contrast, the semicrystalline BSPEEK45 membrane ( $X_c = 14.4\%$ ) is mechanically stable with a more controlled water uptake at almost half the water content of the random analogue.

## CONCLUSIONS

In this work, a simple postpolymerization technique to create blocky SPEEK ionomers has been demonstrated. By sulfonating in the heterogeneous gel state, sulfonation is restricted to the solvent swollen amorphous fraction, which preserves long “blocks” of crystallizable pure PEEK chain segments in the resulting blocky ionomer. Evidence of the blocky architecture was provided by analysis of the SPEEK  $T_g$ 's. While random SPEEK displayed a  $T_g$  that increased with increasing degree of sulfonation, blocky SPEEK exhibited a  $T_g$  that was independent of degree of sulfonation above 7.6% sulfonated, consistent with the blocky architecture. Further analysis of the thermal transitions demonstrated that the blocky architecture leads to enhanced crystallizability and less significant melting point depression as compared to random copolymers. Even at ion contents as low as 3.6%, the blocky SPEEK demonstrated higher crystallizability and significantly faster crystallization kinetics than random SPEEK. Additionally, membranes cast from the low ion-content blocky and random SPEEK displayed similar water uptake and swelling that was dependent on degree of sulfonation. Despite the similar water content, blocky SPEEK membranes exhibited higher proton conductivity than random SPEEK membranes attributed to a somewhat higher ion content in the amorphous phase (due to increased crystallinity) and perhaps a more interconnected network of ionic aggregates. For SPEEK membranes of significantly higher ionic content, the

conductivity of the blocky membranes was significantly greater than the random analogues and even rivaled that of the benchmark Nafion. Overall, this study demonstrated that sulfonation of PEEK in the gel state provides a facile method to produce blocky functional copolymers with high ion content, high crystallizability, and profoundly higher conductivity than that of conventionally sulfonated PEEK.

## ASSOCIATED CONTENT

### Supporting Information

The Supporting Information is available free of charge on the ACS Publications website at DOI: 10.1021/acs.macromol.8b01152.

Figure S1: TGA of PEEK, H<sup>+</sup>-SPEEK, Na<sup>+</sup>-SPEEK, and Cs<sup>+</sup>-SPEEK; Figure S2: <sup>1</sup>H NMR integration of SPEEK samples; Figure S3: <sup>1</sup>H NMR analysis of random SPEEK45 in DMSO-*d*<sub>6</sub> and DCA/CDCl<sub>3</sub>; Figure S4: comparison of <sup>1</sup>H NMR spectra of random SPEEK 45 in DMSO-*d*<sub>6</sub>, DCA/CDCl<sub>3</sub>, and DCA/DMSO-*d*<sub>6</sub>; Table S1: elemental analysis of random SPEEK; Figure S5: percent crystallinity following 2 h isothermal crystallization; Table S2: thermal transitions from DSC; Figure S6: fractional crystallinity versus ln(*t*) at various crystallization temperatures; Table S3: kinetic parameters from Avrami analysis; Table S4: crystallinity of as-cast membranes; Figure S7: fit of USAXS/SAXS data for RSPEEK membranes; Figure S8: fit of ionomer peak for quenched SPEEK; Table S5: multiplet radii of RSPEEK membranes; Figure S9: USAXS/SAXS/WAXS of sulfonated syndiotactic polystyrene (PDF)

## AUTHOR INFORMATION

### Corresponding Author

\*(R.B.M.) E-mail [rbmoore3@vt.edu](mailto:rbmoore3@vt.edu); Ph (540) 231-6015; Fax (540) 231-8517.

### ORCID

Lindsey J. Anderson: 0000-0002-6203-6805

Gregory B. Fahs: 0000-0002-4400-6995

Robert B. Moore: 0000-0001-9057-7695

### Notes

The authors declare no competing financial interest.

## ACKNOWLEDGMENTS

This material is based upon work supported by the National Science Foundation under Grants DMR-1507245 and DMR-1809291 and by Solvay Specialty Polymers. This research used resources of the Advanced Photon Source (APS) and a U.S. Department of Energy (DOE) Office of Science User Facility operated for the DOE Office of Science by Argonne National Laboratory under General User Proposal Number 49574. USAXS/SAXS/WAXD data were collected on the 9-ID-C beamline at the APS, Argonne National Laboratory.

## REFERENCES

- (1) Xing, P.; Robertson, G. P.; Guiver, M. D.; Mikhailenko, S. D.; Wang, K.; Kaliaguine, S. Synthesis and characterization of sulfonated poly(ether ether ketone) for proton exchange membranes. *J. Membr. Sci.* **2004**, 229 (1–2), 95–106.
- (2) Shi, Z.; Holdcroft, S. Synthesis and Proton Conductivity of Partially Sulfonated Poly([vinylidene difluoride-co-hexafluoropropylene]-*b*-styrene) Block Copolymers. *Macromolecules* **2005**, 38 (10), 4193–4201.

- (3) Drioli, E.; Regina, A.; Casciola, M.; Oliveti, A.; Trotta, F.; Massari, T. Sulfonated PEEK-WC membranes for possible fuel cell applications. *J. Membr. Sci.* **2004**, *228* (2), 139–148.
- (4) Chen, Y.; Guo, R.; Lee, C. H.; Lee, M.; McGrath, J. E. Partly fluorinated poly(arylene ether ketone sulfone) hydrophilic–hydrophobic multiblock copolymers for fuel cell membranes. *Int. J. Hydrogen Energy* **2012**, *37* (7), 6132–6139.
- (5) Mauritz, K. A.; Moore, R. B. State of Understanding of Nafion. *Chem. Rev.* **2004**, *104* (10), 4535–4586.
- (6) Eisenberg, A.; Hird, B.; Moore, R. B. A new multiplet-cluster model for the morphology of random ionomers. *Macromolecules* **1990**, *23* (18), 4098–4107.
- (7) Hsu, W. Y.; Gierke, T. D. Ion transport and clustering in nafion perfluorinated membranes. *J. Membr. Sci.* **1983**, *13* (3), 307–326.
- (8) Gierke, T. D.; Munn, G. E.; Wilson, F. C. The morphology in nafion perfluorinated membrane products, as determined by wide- and small-angle x-ray studies. *J. Polym. Sci., Polym. Phys. Ed.* **1981**, *19* (11), 1687–1704.
- (9) Kusoglu, A.; Weber, A. Z. New Insights into Perfluorinated Sulfonic-Acid Ionomers. *Chem. Rev.* **2017**, *117* (3), 987–1104.
- (10) Chang, Y.; Lee, Y.-B.; Bae, C. Partially fluorinated sulfonated poly(ether amide) fuel cell membranes: influence of chemical structure on membrane properties. *Polymers* **2011**, *3* (1), 222–235.
- (11) Swier, S.; Chun, Y. S.; Gasa, J.; Shaw, M. T.; Weiss, R. A. Sulfonated poly(ether ketone ketone) ionomers as proton exchange membranes. *Polym. Eng. Sci.* **2005**, *45* (8), 1081–1091.
- (12) Osborn, A. M. *Investigation of Phase Morphology and Blend Stability in Ionomeric Perfluorocyclobutane (PFCB)/Poly(vinylidene difluoride) (PVDF) Copolymer Blend Membranes*; Virginia Tech: Blacksburg, VA, 2010.
- (13) Hickner, M. A.; Ghassemi, H.; Kim, Y. S.; Einsla, B. R.; McGrath, J. E. Alternative Polymer Systems for Proton Exchange Membranes (PEMs). *Chem. Rev.* **2004**, *104* (10), 4587–4612.
- (14) Knauth, P.; Di Vona, M. L. Sulfonated aromatic ionomers: Analysis of proton conductivity and proton mobility. *Solid State Ionics* **2012**, *225*, 255–259.
- (15) Di Vona, M. L.; Sgreccia, E.; Licoccia, S.; Alberti, G.; Tortet, L.; Knauth, P. Analysis of Temperature-Promoted and Solvent-Assisted Cross-Linking in Sulfonated Poly(ether ether ketone) (SPEEK) Proton-Conducting Membranes. *J. Phys. Chem. B* **2009**, *113* (21), 7505–7512.
- (16) Zhang, G.; Fu, T.; Wu, J.; Li, X.; Na, H. Synthesis and characterization of a new type of sulfonated poly(ether ether ketone)s for proton exchange membranes. *J. Appl. Polym. Sci.* **2010**, *116* (3), 1515–1523.
- (17) Knauth, P.; Hou, H.; Bloch, E.; Sgreccia, E.; Di Vona, M. L. Thermogravimetric analysis of SPEEK membranes: Thermal stability, degree of sulfonation and cross-linking reaction. *J. Anal. Appl. Pyrolysis* **2011**, *92* (2), 361–365.
- (18) Rikukawa, M.; Sanui, K. Proton-conducting polymer electrolyte membranes based on hydrocarbon polymers. *Prog. Polym. Sci.* **2000**, *25* (10), 1463–1502.
- (19) Higashihara, T.; Matsumoto, K.; Ueda, M. Sulfonated aromatic hydrocarbon polymers as proton exchange membranes for fuel cells. *Polymer* **2009**, *50* (23), 5341–5357.
- (20) Reyes-Rodriguez, J. L.; Solorza-Feria, O.; Garcia-Bernabe, A.; Gimenez, E.; Sahuquillo, O.; Compan, V. Conductivity of composite membrane-based poly(ether-ether-ketone) sulfonated (SPEEK) nanofiber mats of varying thickness. *RSC Adv.* **2016**, *6* (62), 56986–56999.
- (21) Lee, J. K.; Li, W.; Manthiram, A. Sulfonated poly(ether ether ketone) as an ionomer for direct methanol fuel cell electrodes. *J. Power Sources* **2008**, *180* (1), 56–62.
- (22) Kaliaguine, S.; Mikhailenko, S.; Wang, K.; Xing, P.; Robertson, G.; Guiver, M. Properties of SPEEK based PEMs for fuel cell application. *Catal. Today* **2003**, *82* (1), 213–222.
- (23) Bailly, C.; Williams, D. J.; Karasz, F. E.; MacKnight, W. J. The sodium salts of sulphonated poly(aryl-ether-ether-ketone) (PEEK): Preparation and characterization. *Polymer* **1987**, *28* (6), 1009–1016.
- (24) Seo, D. W.; Lim, Y. D.; Lee, S. H.; Hossain, M. A.; Islam, M. M.; Lee, H. C.; Jang, H. H.; Kim, W. G. Preparation and characterization of block copolymers containing multi-sulfonated unit for proton exchange membrane fuel cell. *Electrochim. Acta* **2012**, *86*, 352–359.
- (25) Meier-Haack, J.; Taeger, A.; Vogel, C.; Schlenstedt, K.; Lenk, W.; Lehmann, D. Membranes from sulfonated block copolymers for use in fuel cells. *Sep. Purif. Technol.* **2005**, *41* (3), 207–220.
- (26) Yu, X.; Roy, A.; Dunn, S.; Badami, A. S.; Yang, J.; Good, A. S.; McGrath, J. E. Synthesis and characterization of sulfonated-fluorinated, hydrophilic-hydrophobic multiblock copolymers for proton exchange membranes. *J. Polym. Sci., Part A: Polym. Chem.* **2009**, *47* (4), 1038–1051.
- (27) Lee, M.; Park, J. K.; Lee, H.-S.; Lane, O.; Moore, R. B.; McGrath, J. E.; Baird, D. G. Effects of block length and solution-casting conditions on the final morphology and properties of disulfonated poly(arylene ether sulfone) multiblock copolymer films for proton exchange membranes. *Polymer* **2009**, *50* (25), 6129–6138.
- (28) Roy, A.; Hickner, M. A.; Yu, X.; Li, Y.; Glass, T. E.; McGrath, J. E. Influence of chemical composition and sequence length on the transport properties of proton exchange membranes. *J. Polym. Sci., Part B: Polym. Phys.* **2006**, *44* (16), 2226–2239.
- (29) Zhao, C.; Li, X.; Wang, Z.; Dou, Z.; Zhong, S.; Na, H. Synthesis of the block sulfonated poly(ether ether ketone)s (S-PEEKs) materials for proton exchange membrane. *J. Membr. Sci.* **2006**, *280* (1–2), 643–650.
- (30) Zhao, C.; Lin, H.; Shao, K.; Li, X.; Ni, H.; Wang, Z.; Na, H. Block sulfonated poly(ether ether ketone)s (SPEEK) ionomers with high ion-exchange capacities for proton exchange membranes. *J. Power Sources* **2006**, *162* (2), 1003–1009.
- (31) Chen, Y.; Lee, C. H.; Rowlett, J. R.; McGrath, J. E. Synthesis and characterization of multiblock semi-crystalline hydrophobic poly(ether ether ketone)–hydrophilic disulfonated poly(arylene ether sulfone) copolymers for proton exchange membranes. *Polymer* **2012**, *53* (15), 3143–3153.
- (32) Yang, A. C. C.; Narimani, R.; Frisken, B. J.; Holdcroft, S. Investigations of crystallinity and chain entanglement on sorption and conductivity of proton exchange membranes. *J. Membr. Sci.* **2014**, *469*, 251–261.
- (33) Hamada, T.; Hasegawa, S.; Fukasawa, H.; Sawada, S.-i.; Koshikawa, H.; Miyashita, A.; Maekawa, Y. Poly(ether ether ketone) (PEEK)-based graft-type polymer electrolyte membranes having high crystallinity for high conducting and mechanical properties under various humidified conditions. *J. Mater. Chem. A* **2015**, *3* (42), 20983–20991.
- (34) Wang, R.; Yan, X.; Wu, X.; He, G.; Du, L.; Hu, Z.; Tan, M. Modification of hydrophilic channels in Nafion membranes by DMBA: Mechanism and effects on proton conductivity. *J. Polym. Sci., Part B: Polym. Phys.* **2014**, *52* (16), 1107–1117.
- (35) Gao, X.; Liu, Y.; Li, J. Review on Modification of Sulfonated Poly(-ether-ether-ketone) Membranes Used as Proton Exchange Membranes. *Mater. Sci.* **2015**, *21* (4), 574–582.
- (36) Fahs, G. B.; Benson, S. D.; Moore, R. B. Blocky Sulfonation of Syndiotactic Polystyrene: A Facile Route toward Tailored Ionomer Architecture via Postpolymerization Functionalization in the Gel State. *Macromolecules* **2017**, *50* (6), 2387–2396.
- (37) Benson, S. D. The Effect of Nanoscale Particles and Ionomer Architecture on the Crystallization Behavior of Sulfonated Syndiotactic Polystyrene. Ph.D. Dissertation, Virginia Polytechnic Institute and State University, Blacksburg, VA, 2010.
- (38) Talley, S. J.; Yuan, X.; Moore, R. B. Thermoreversible Gelation of Poly(ether ether ketone). *ACS Macro Lett.* **2017**, *6* (3), 262–266.
- (39) Corby, B. W.; Gray, A. D.; Meaney, P. J.; Falvey, M. J.; Lawrence, G. P.; Smyth, T. P. Clean-chemistry sulfonation of aromatics. *J. Chem. Res.* **2002**, *2002* (7), 326–327.
- (40) Bakker, B. H.; Cerfontain, H. Sulfonation of Alkenes by Chlorosulfuric Acid, Acetyl Sulfate, and Trifluoroacetyl Sulfate. *Eur. J. Org. Chem.* **1999**, *1999* (1), 91–96.

- (41) Koziara, B. T.; Kappert, E. J.; Ogieglo, W.; Nijmeijer, K.; Hempenius, M. A.; Benes, N. E. Thermal Stability of Sulfonated Poly(Ether Ether Ketone) Films: on the Role of Protodesulfonation. *Macromol. Mater. Eng.* **2016**, *301* (1), 71–80.
- (42) Ilavsky, J.; Jemian, P. R. Ultra-small-angle X-ray scattering at the Advanced Photon Source. *J. Appl. Crystallogr.* **2009**, *42* (3), 469–479.
- (43) Ilavsky, J.; Jemian, P. R. Irena: tool suite for modeling and analysis of small-angle scattering. *J. Appl. Crystallogr.* **2009**, *42*, 347–353.
- (44) Ilavsky, J. Nika: software for two-dimensional data reduction. *J. Appl. Crystallogr.* **2012**, *45* (2), 324–328.
- (45) Banerjee, S.; Kar, K. K. Impact of degree of sulfonation on microstructure, thermal, thermomechanical and physicochemical properties of sulfonated poly ether ether ketone. *Polymer* **2017**, *109*, 176–186.
- (46) Iulianelli, A.; Basile, A. Sulfonated PEEK-based polymers in PEMFC and DMFC applications: a review. *Int. J. Hydrogen Energy* **2012**, *37* (20), 15241–15255.
- (47) Huang, R. Y. M.; Shao, P.; Burns, C. M.; Feng, X. Sulfonation of poly(ether ether ketone)(PEEK): Kinetic study and characterization. *J. Appl. Polym. Sci.* **2001**, *82* (11), 2651–2660.
- (48) Weiss, R. A.; Turner, S. R.; Lundberg, R. D. Sulfonated polystyrene ionomers prepared by emulsion copolymerization of styrene and sodium styrene sulfonate. *J. Polym. Sci., Polym. Chem. Ed.* **1985**, *23* (2), 525–533.
- (49) Weiss, R. A.; Lundberg, R. D.; Turner, S. R. Comparisons of styrene ionomers prepared by sulfonating polystyrene and copolymerizing styrene with styrene sulfonate. *J. Polym. Sci., Polym. Chem. Ed.* **1985**, *23* (2), 549–568.
- (50) Blundell, D. J.; Osborn, B. N. The morphology of poly(aryl-ether-ether-ketone). *Polymer* **1983**, *24* (8), 953–958.
- (51) Tan, S.; Su, A.; Luo, J.; Zhou, E. Crystallization kinetics of poly(ether ether ketone) (PEEK) from its metastable melt. *Polymer* **1999**, *40* (5), 1223–1231.
- (52) Verma, R. K.; Velikov, V.; Kander, R. G.; Marand, H.; Chu, B.; Hsiao, B. S. SAXS studies of lamellar level morphological changes during crystallization and melting in PEEK. *Polymer* **1996**, *37* (24), 5357–5365.
- (53) Chen, H.-L.; Porter, R. S. Melting behavior of poly(ether ether ketone) in its blends with poly(ether imide). *J. Polym. Sci., Part B: Polym. Phys.* **1993**, *31* (12), 1845–1850.
- (54) Flory, P. J. Theory of crystallization in copolymers. *Trans. Faraday Soc.* **1955**, *51* (0), 848–857.
- (55) Flory, P. J. Thermodynamics of Crystallization in High Polymers II. Simplified Derivation of Melting-Point Relationships. *J. Chem. Phys.* **1947**, *15* (9), 684–684.
- (56) Orler, E. B.; Moore, R. B. Influence of Ionic Interactions on the Crystallization of Lightly Sulfonated Syndiotactic Polystyrene Ionomers. *Macromolecules* **1994**, *27* (17), 4774–4780.
- (57) Orler, E. B.; Calhoun, B. H.; Moore, R. B. Crystallization Kinetics as a Probe of the Dynamic Network in Lightly Sulfonated Syndiotactic Polystyrene Ionomers. *Macromolecules* **1996**, *29* (18), 5965–5971.
- (58) Gebel, G. Structure of Membranes for Fuel Cells: SANS and SAXS Analyses of Sulfonated PEEK Membranes and Solutions. *Macromolecules* **2013**, *46* (15), 6057–6066.
- (59) Song, J.-M.; Shin, J.; Sohn, J.-Y.; Nho, Y. C. Ionic aggregation characterization of sulfonated PEEK ionomers using by X-ray and DMA techniques. *Macromol. Res.* **2012**, *20* (5), 477–483.
- (60) Crevecoeur, G.; Groeninckx, G. Binary blends of poly(ether ether ketone) and poly(ether imide): miscibility, crystallization behavior and semicrystalline morphology. *Macromolecules* **1991**, *24* (5), 1190–1195.
- (61) Verma, R.; Marand, H.; Hsiao, B. Morphological Changes during Secondary Crystallization and Subsequent Melting in Poly(ether ether ketone) as Studied by Real Time Small Angle X-ray Scattering. *Macromolecules* **1996**, *29* (24), 7767–7775.
- (62) Yang, B.; Manthiram, A. Comparison of the small angle X-ray scattering study of sulfonated poly(etheretherketone) and Nafion membranes for direct methanol fuel cells. *J. Power Sources* **2006**, *153* (1), 29–35.
- (63) Luu, D. X.; Cho, E.-B.; Han, O. H.; Kim, D. SAXS and NMR Analysis for the Cast Solvent Effect on sPEEK Membrane Properties. *J. Phys. Chem. B* **2009**, *113* (30), 10072–10076.
- (64) Kawaguti, C. A.; Dahmouche, K.; Gomes, A. d. S. Nanostructure and properties of proton-conducting sulfonated poly(ether ether ketone) (SPEEK) and zirconia–SPEEK hybrid membranes for direct alcohol fuel cells: effect of the nature of swelling solvent and incorporation of heteropolyacid. *Polym. Int.* **2012**, *61* (1), 82–92.
- (65) Smitha, B.; Sridhar, S.; Khan, A. A. Solid polymer electrolyte membranes for fuel cell applications—a review. *J. Membr. Sci.* **2005**, *259* (1), 10–26.
- (66) Li, Q.; He, R.; Jensen, J. O.; Bjerrum, N. J. Approaches and Recent Development of Polymer Electrolyte Membranes for Fuel Cells Operating above 100 °C. *Chem. Mater.* **2003**, *15* (26), 4896–4915.
- (67) Peighambaridoust, S. J.; Rowshanzamir, S.; Amjadi, M. Review of the proton exchange membranes for fuel cell applications. *Int. J. Hydrogen Energy* **2010**, *35* (17), 9349–9384.
- (68) Hickner, M. A.; Pivovar, B. S. The Chemical and Structural Nature of Proton Exchange Membrane Fuel Cell Properties. *Fuel Cells* **2005**, *5* (2), 213–229.
- (69) Peckham, T. J.; Schmeisser, J.; Rodgers, M.; Holdcroft, S. Main-chain, statistically sulfonated proton exchange membranes: the relationships of acid concentration and proton mobility to water content and their effect upon proton conductivity. *J. Mater. Chem.* **2007**, *17* (30), 3255–3268.
- (70) Elabd, Y. A.; Hickner, M. A. Block Copolymers for Fuel Cells. *Macromolecules* **2011**, *44* (1), 1–11.